Pergamon

Geochimica et Cosmochimica Acta, Vol. 67, No. 12, pp. 2137–2146, 2003
Copyright © 2003 Elsevier Science Ltd
Printed in the USA. All rights reserved
0016-7037/03 $30.00 + .00

doi:10.1016/S0016-7037(02)01371-6

Surface oxidation of chalcopyrite ($CuFeS_2$) under ambient atmospheric and aqueous (pH 2-10) conditions: Cu, Fe L- and O K-edge X-ray spectroscopy

E. C. Todd,[1] D. M. Sherman,[1,*] and J. A. Purton[2]

[1]Department of Earth Sciences, University of Bristol, Bristol, United Kingdom
[2]Daresbury Laboratory, Warrington, United Kingdom

(*Received July* 16, 2002; *accepted in revised form November* 11, 2002)

Abstract—X-ray absorption and emission spectra were used to characterize the surface of chalcopyrite after oxidation both in air and in air-saturated aqueous solution (pH = 2–10). For chalcopyrite oxidized in aqueous solution, the Cu and Fe L-edge spectra show that the surface oxidation layer is copper deficient. As the pH increases, O K-edge spectra reveal a change in the nature of the oxidation layer. An iron (hydroxy)sulfate is dominant at low pH, whereas FeOOH is the major surface phase under alkaline conditions. Fe_2O_3 may be present at intermediate pH. The surfaces of chalcopyrite samples oxidized in air consist of a mixture of copper oxides, FeOOH, and sulfate phases. Sulfate is much more abundant on the surface of air-oxidized chalcopyrite because of its high solubility in aqueous solution. Likewise, copper oxidation products can be observed in the O K-edge spectra of air-oxidized chalcopyrite in contrast to the aqueous samples. *Copyright © 2003 Elsevier Science Ltd*

1. INTRODUCTION

Chalcopyrite ($CuFeS_2$) is an important ore mineral of copper and an accessory mineral in many igneous rocks. The surface oxidation layer of chalcopyrite controls its environmental chemistry and behavior during ore-flotation processes. The surface oxidation of chalcopyrite in aqueous solution has been studied using electrochemical methods (Gardner and Woods, 1979; Zachwieja et al., 1989; Yin et al., 1995; Velasquez et al., 1998). Velasquez et al. (1998) explained their electrochemical and XPS data for chalcopyrite oxidation at pH 9.2 by the formation of Fe_2O_3 and FeOOH iron products, as well as CuO, CuFeO, and CuS. Yin et al. (1995) found that electrochemical oxidation of chalcopyrite depends on pH, with the formation of sulfate under acidic conditions being replaced by that of iron oxide or hydroxide as the pH increased. Gardner and Woods (1979) also observed that ferric hydroxide is a major surface product of chalcopyrite oxidation at basic and neutral pH. The formation of a hydrated iron oxyhydroxide layer and an iron-deficient chalcopyrite lattice in air-saturated alkaline solutions was confirmed by Zachwieja et al. (1989).

X-ray spectroscopy can characterize sulfide mineral surfaces at the molecular level. A number of studies have used X-ray photoelectron spectroscopy (XPS) to identify elements and their oxidation states on the chalcopyrite surface (Gardner and Woods, 1979; Brion, 1980; Buckley and Woods, 1984; Luttrell and Yoon, 1984; Zachwieja et al., 1989; Mielczarski et al., 1996; Grano et al., 1997; Velasquez et al., 1998; Pratesi and Cipriani, 2000). Auger electron spectroscopy has also been used as a supplementary technique (Pratesi and Cipriani, 2000). Most authors have concluded that iron (oxyhydr)oxides are the main surface oxidation phase. Grano et al. (1997), Mielczarski et al. (1996), and Brion (1980) all find that there are insignificant amounts of copper oxides at the mineral surface. An iron-enriched upper surface is thought to be underlain by a CuS and/or CuS_2 layer (Buckley and Woods, 1984). Velasquez et al. (1998), however, explained their electrochemical and XPS data for chalcopyrite oxidation at pH 9.2 by the formation of CuO, CuFeO, plus CuS (as well as Fe_2O_3 and FeOOH) on the surface. Generally there has been little or no evidence for sulfate on the surface of chalcopyrite oxidized in aqueous solution (Grano et al., 1997; Velasquez, 1998). Iron and copper sulfates, however, have been observed after oxidation of chalcopyrite in air (Buckley and Woods, 1984; Pratesi and Cipriani, 2000). Other XPS studies provide evidence for the presence of monosulfide, polysulfide, and thiosulfate intermediates (Mielczarski et al., 1996; Pratesi and Cipriani, 2000), depending on the duration of oxidation.

The Eh-pH diagrams for the Cu-Fe-S system (Fig. 1) are consistent with some of these researchers' observations. There is no region in which we predict sulfate precipitates, although natrojarosite is metastable at low pH. At high pH, we would expect the formation of a CuO phase on the surface. An Eh gradient with depth might give metastable layers of Cu_2O, Cu, and Cu_2S.

In this study, we use X-ray absorption (XAS) and emission (XES) spectroscopy to provide new insights into the surface oxidation of chalcopyrite. The advantage of these techniques over XPS is that we can determine the presence of chemical bonds and hence identify the surface oxidation phase. XAS probes the unoccupied density of states and has already been used to study the electronic structure and nature of bonding in chalcopyrite (Li et al., 1994a,b). The Cu L-edge spectra can characterize the oxidation state of copper in sulfide minerals (Grioni et al., 1989; Pattrick et al., 1993, 1997; van der Laan et al., 1992), but they have yet to be used in a systematic inves-

* Author to whom correspondence should be addressed (dave.sherman@bris.ac.uk).

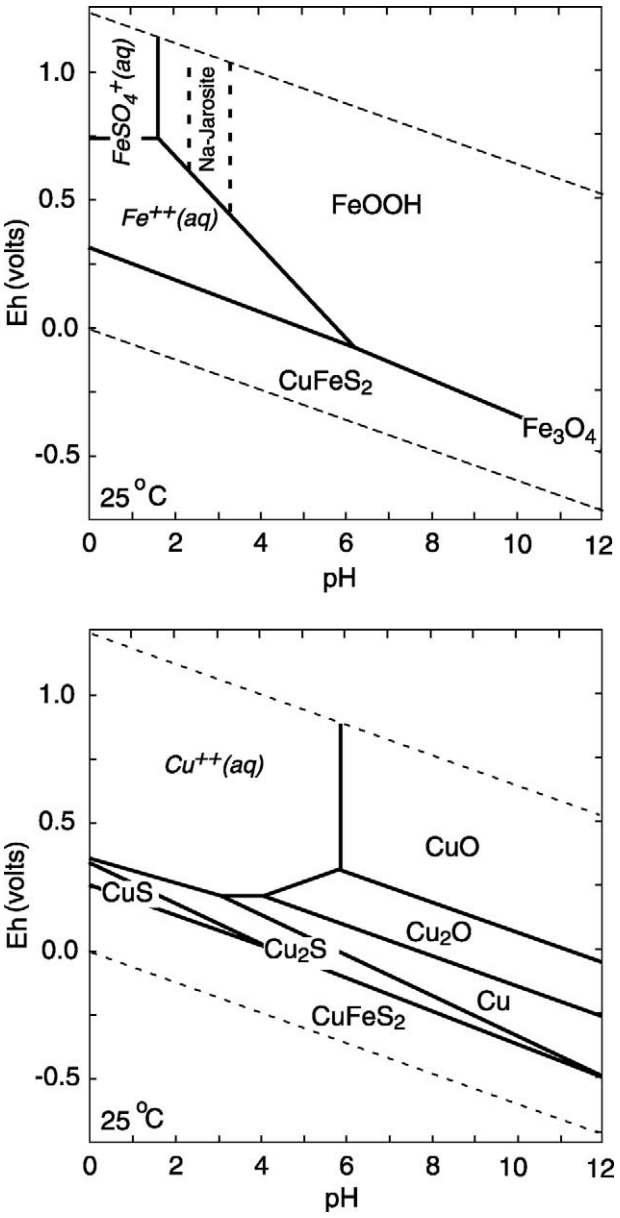

Fig. 1. (a) Eh-pH diagram for the Fe-S system. (b) Eh-pH diagram for the Cu-S system. Concentrations: 1×10^{-4}M copper and iron, 2×10^{-4}M sulfur total in 0.1M Na^+. Aqueous species data from Wagman et al. (1982). Mineral data from Helgeson et al. (1978). Metastable stability field of natrojarosite calculated by suppressing goethite formation.

tigation of the oxidation of sulfide surfaces. As we show here, the oxygen K-edge XAS are useful for identifying surface oxide and sulfate phases.

Whereas X-ray absorption spectroscopy probes the unoccupied electronic states, X-ray emission samples the occupied states as electrons fall into the empty core levels of the excited state. Combining the information from X-ray emission and X-ray absorption spectra taken for the same mineral gives a complete picture of its electronic structure. In addition, use of tunable synchrotron radiation for XES allows atoms at inequivalent sites to be identified. For example, different types of oxygen environments (oxide vs. hydroxide) can be resolved.

2. EXPERIMENTAL METHODS

2.1. Sample Preparation

Chalcopyrite samples from the University of Bristol museum collection were characterized using XRD to ensure that the samples were single phases. Samples were coarsely ground in a nitrogen glove box then immersed in air-saturated 0.1-M sodium nitrate solutions for 7 days. The pH of the aqueous electrolyte was adjusted initially and also once during the equilibration period using 0.1-M nitric acid and 0.1-M sodium hydroxide. The final values were established to range between pH 1.85 and 10.67. The samples were dried and stored under N_2 before being mounted on stainless steel sample holders using carbon tape. All procedures were carried out under nitrogen to ensure that the only oxidation products were those formed in aqueous solution. A sample ground and stored under nitrogen was retained as a control. The oxidation of chalcopyrite in air was also studied. Samples were exposed to ambient atmosphere (T = 20ºC, $P_{H2O} \sim 0.02$ bar) for at least 1 week. Spectra were obtained in vacuo.

2.2. X-Ray Absorption and Emission Spectroscopy

Cu, S, Fe L-edge, and O K-edge X-ray absorption spectra were measured at station I51 of the Max-II Synchrotron Radiation Source, Lund, Sweden, for a range of samples conditioned in aqueous solution. Complementary data for two chalcopyrite samples oxidized in air were also recorded at station 5U.1 of Daresbury Laboratory, United Kingdom. Bulk-like spectra were obtained by using argon sputtering to remove any surface oxidation phase. All XAS spectra were collected using the total electron yield (TEY) method to measure the drain current. The mean probing depth in the TEY mode is 20 to 50 Å (Abbate et al., 1992), although the analysis depth varies somewhat with energy. Kasrai et al. (1996), for example, found that the maximum probing depth in the TEY mode at the Si L-edge (95–120 eV) is ~50 Å, compared with ~700 Å at the Si K-edge (1830–1900 eV). For this reason, we might expect to see some bulk contribution at the metal L-edges where samples are only mildly oxidized. The S L-edge, however, will be surface sensitive. The O K-edge can, of course, only sample the surface oxidation layer because there is no oxygen in the bulk sulfide substrate.

To correct for synchrotron-intensity loss during measurement, the XAS spectra were normalized by dividing the signal, I, by the reference I_0, where I_0 is the intensity of the photon flux and I is the total electron yield.

O K-XES data were also collected at Max-II. The excitation energies of the emission spectra were varied to study specific features in the corresponding XAS spectra. The XAS and XES data were aligned by comparing the position of the elastic peak in the XES with the excitation energy (as selected from the XAS spectra).

3. RESULTS AND DISCUSSION

3.1. X-Ray Absorption Spectra of Unoxidized Chalcopyrite

The Cu, Fe, and S L-edges of pristine chalcopyrite are shown in Figure 2. Peak energies and assignments are summarized in Tables 1 and 2. The copper L-edge (Fig. 2A) is consistent with the results of Grioni et al. (1989b), Pattrick et al. (1993, 1997), and van der Laan et al. (1992). The sulfur L-edge (Fig. 2B) is comparable to that of Li et al. (1994). Our interpretation of the Cu L-edge, however, is different from that of other authors. The formal electronic charge configuration in chalcopyrite, as indicated by neutron diffraction and Mossbauer studies (Vaughan and Craig, 1978), has been argued to be $Cu^+Fe^{3+}S_2$. Pre-edge features in the Cu L-edge spectra result from transitions from the Cu (2p) states to vacant levels with Cu (3d) character;

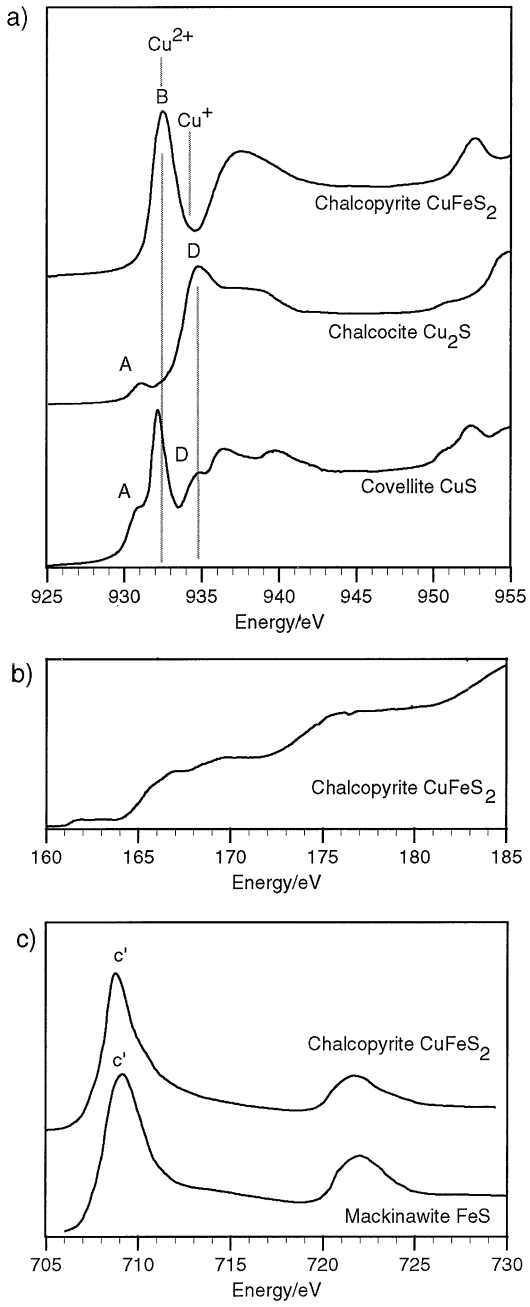

Fig. 2. (a) The Cu L-edges of pristine chalcopyrite, $CuFeS_2$, chalcocite, Cu_2S, and covellite CuS. Peak A is Cu (II)-O contamination. Peak B corresponds to excitations to unoccupied 3d-like states of Cu (II)-S. Peak D shows the transition to the 3d-4s like states of Cu (I)-S. (b) The S L-edge of chalcopyrite. (c) The Fe L-edges of chalcopyrite and mackinawite. The spectra both show Fe (II) in tetrahedral coordination.

hence, there are no allowed transitions in the case of Cu (I), which has a filled d^{10} configuration. A Cu L-edge spectrum is, however, obtained for Cu (I) because of d-character in the 4s states (giving features in the energy region above the pre-edge), although the transition probability is low. On this basis, we would not expect to see a pre-edge feature for chalcopyrite as $Cu^+Fe^{3+}S_2$. The spectrum shows a strong peak (B) at 932.4 eV representing excitations to empty 3d-states, however. This is not compatible with the presence of purely monovalent copper. Comparison of the peak position with those of the copper sulfides, chalcocite [all Cu (I)], and covellite [Cu (II) and Cu (I)] shows that the valence state of copper in chalcopyrite is Cu (II) (see Fig. 2a). Chalcocite has no peak in the region near 932 eV, indicating that it has a Cu (I) or d^{10} configuration. Covellite, on the other hand, has a strong peak (B) at 932.2 eV, representing Cu (II) bonded to sulfur. There is also a contribution from the 3d-4s states of Cu (I) at 935 eV (peak D) consistent with the presence of Cu (I). The pre-edge feature (peak B) at 932.4 eV in the Cu L-edge of chalcopyrite can only be explained by the presence of Cu (II) in the mineral structure, i.e., a $Cu^{2+}Fe^{2+}S_2$ configuration.

The iron L-edge (Fig 2c) supports the $Cu^{2+}Fe^{2+}S_2$ configuration. The Fe L-edge of chalcopyrite is the same as that of mackinawite (FeS), which contains Fe (II) in tetrahedral coordination with S^{2-}. The Fe L_3- and L_2-edges are single peaks, although in high-spin iron compounds the d-orbitals are split because of excitations to the partially occupied t_{2g}- and e_g-like states. The single peaks in the Fe L-edge of chalcopyrite may reflect the small tetrahedral crystal field splitting energy, which is about half that of the equivalent splitting in an octahedral field, meaning that the two features are simply not resolved.

3.2. Effect of pH on Aqueous Chalcopyrite Oxidation

3.2.1. XAS spectroscopy

Cu, Fe, and S L-edge, and O K-edge spectra were collected for each of five chalcopyrite samples reacted in air-saturated sodium nitrate solutions at pH = 1.85 to 10.67. The Cu L-edge spectra of the aqueous samples (Fig. 3) show little variation with pH, other than that the spectra become noisier and the signal intensity decreases as the pH tends toward alkaline. Comparison of the spectra with those taken for a sample cleaved in N_2, and also for other chalcopyrite samples whose surfaces were "cleaned" using argon sputtering, reveal that the Cu L-edge corresponds to that of the unoxidized mineral. The uniformity of the spectra, even as pH is altered, suggests that either the Cu L-edge is sampling only the bulk mineral or that the copper component of chalcopyrite remains relatively unchanged during aqueous oxidation. Mielczarski et al. (1996) observed various ferric and ferrous oxides and hydroxides on chalcopyrite surfaces but found an insignificant amount of copper oxidation species. Brion (1980) also found that, after exposure of freshly ground chalcopyrite to distilled water, the only change is the formation of Fe oxyhydroxide or hydroxide within the first layers of $CuFeS_2$. Grano et al. (1997) suggested that copper remains bonded to sulfur and ruled out the presence of copper oxides on the basis that the Cu(2p) spectrum showed only the characteristic chalcopyrite peaks. Grano et al. also attributed all oxide components to iron rather than copper oxides and confirmed an absence of any aqueous copper species in the supernatant solutions. Our data similarly suggest that Cu is not present in the oxidation layer. The noisiness of the alkaline samples may indicate the presence of a thick iron (oxyhydr)oxide coating, diminishing the Cu signal.

Unlike the Cu L-edges, the Fe L-edges of chalcopyrite (Fig.

Table 1. Peak energies and assignments in Cu L-edge spectra.

Peak	Energy/eV	Peak Assignment	Example minerals
A	931.4 eV	Cu (2p) ⇒ Cu (3d)-like states in Cu (II)-O	Tenorite Air oxidation chalcopyrite Air oxidation copper sulfides.
B	932.3–932.4 eV	Cu (2p) ⇒ Cu (3d)-like states in Cu (II)-S	Covellite, bulk chalcopyrite
C	933.6 eV	Cu (2p) ⇒ Cu (3d, 4s)-like states in Cu(I)-O	Cuprite Air oxidation chalcopyrite
D	934.6 eV	Cu (2p) ⇒ Cu (3d, 4s)-like states in Cu(I)-S	Chalcocite, covellite

4a) show a marked change between pH 3.28 and 5.25 that results from the formation of a surface oxidation layer. Under strongly acidic conditions, the Fe L_3-edge consists of a single peak (c′) at 708.8 eV. The dominant contribution to the Fe L-edge is from the unoxidized bulk iron. Above pH 3.28 there is an additional peak (a′) at 710.2 eV, the intensity of which increases from pH 5.25 to 10.67. This marks the increasing oxidation of the surface, and the formation of a phase with octahedral ferric iron. Under the most alkaline conditions, the Fe L-edge closely resembles those of the iron (oxyhydr)oxides hematite, α-Fe_2O_3, and goethite, $\alpha-$FeOOH (Fig. 4b). Overall, the changes in the Fe L-edge spectra are showing the progressive oxidation of chalcopyrite from highly acidic conditions (<pH 3.28), where bulk iron is the dominant contributor to the spectrum and the chalcopyrite is only mildly oxidized, to highly alkaline conditions, where the surface iron consists entirely of a ferric oxidation product.

The O K-edge is a much more sensitive probe of surface oxidation products (Table 3) than the metal L-edges, as there can be no bulk contribution to the spectrum. The chalcopyrite sample, cleaved and stored under N_2, has a weak and noisy oxygen spectrum; hence, the surface was nearly pristine. Any oxidation layer on the aqueous samples must have been formed in solution. Under acidic aqueous conditions the O K-edge (Fig. 5a) consists of a single peak (c) in the near-edge region, at 531.9 eV, followed by a broad structure above 535 eV. The single pre-edge feature appears to decrease in relative intensity in going from pH 1.85 to pH 3.28, and by pH 5.25 two additional peaks (a and b) are clearly visible at 530 and 531.2 eV. These peaks correspond to transitions to the t_{2g}-like and e_g Fe (3d)–like states of octahedral ferric iron. As the pH increases further, the peak (c) dominating the acidic samples decreases in relative intensity, becoming completely insignificant at pH 10.67. The broad high-energy structure above 535 eV results from multiple scattering and O (1s) to Fe (4s, 4p) transitions.

The progressive change in the oxygen K-edge of chalcopyrite reflects the changing nature of the surface oxide species with pH. The corresponding change in the Fe L-edge, and uniformity in the Cu L-edge support previous suggestions that iron-oxygen species are the predominant oxidation products. The oxidation phase that forms under acidic conditions is difficult to identify. The O K-edge spectra are similar to those of pyrite prepared under almost identical conditions (this study). Because there is no oxide contribution to the spectrum at low pH, the most likely stable phase is an iron sulfate species. The intensity of the pre-edge peak (c) at 531.9 eV is much weaker than in $CuSO_4$ (Fig. 9b) or $Fe_2(SO_4)_3$ (Fig. 5b), however. The high intensity of this peak in the O K-edge of oxidized pyrite (Todd et al., 2003) was attributed to an Fe-OH bond in the surface phase. Indeed, the energy position of peak c is very similar to that of the hydroxide peak (d) seen in the goethite reference (Fig. 5b). The most likely candidate for the low-pH oxidation product is therefore a ferric (hydroxy)sulfate, such as natrojarosite or hydronium jarosite. Unfortunately, the S L-edges (not shown) are poorly resolved and predominantly show a bulk mineral contribution. Similarly, octahedral ferric iron may not be observed in the Fe L-edges because the spectrum is dominated by contributions from the bulk tetrahedral iron. This is consistent with the surface being only mildly oxidized at low pH.

The intermediate pH samples appear to consist of a mixture of the low and high pH phases. Above pH 5.25, the appearance of peaks a and b marks a change to iron in a ferric (oxyhydr)-oxide. Comparison of the energy positions and intensity ratios of peaks in the chalcopyrite O K-edges at high pH with those of reference ferric minerals (Fig. 5b) reveals that an iron (III) (oxyhydr)oxide, probably goethite, is the dominant surface species on the sample oxidized at pH 10.28. There is also evidence for minor amounts of adsorbed water: the small feature (peak e) discernible at about 534 eV may represent the transition to the O (2p)-H (1s) antibonding orbital of H_2O. The same feature was observed by Myneni (2002) in an XAS study of liquid water. We do not expect H_2O to be an important surface phase on our samples, however, because it will desorb under the ultrahigh vacuum conditions.

Our results are consistent with previous studies: Mielczarski

Table 2. Peak energies and peak assignments in Fe L-edge spectra.

Peak	Energy/eV	Peak Assignment	Example minerals
a′	708.8 eV	Fe (2p) ⇒ t_{2g}-like states of Fe (III)	Hematite, goethite (octahedral ferric oxides) High pH/air oxidation chalcopyrite
b′	710.2 eV	Fe (2p) ⇒ e_g-like states of Fe (III)	Hematite, goethite (octahedral ferric oxides) High pH/air oxidation chalcopyrite
c′	708.8 eV	Fe (2p) ⇒ 3d-like states of Fe (II)	Chalcopyrite, mackinawite (tetrahedral ferrous sulfides)

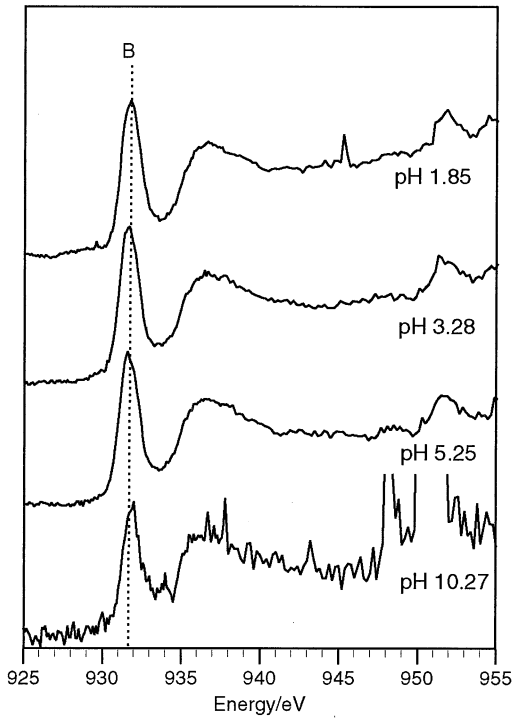

Fig. 3. The Cu L-edges of a series of chalcopyrite samples conditioned in $NaNO_3$ electrolyte at a range of pH. The spectra are uniform in shape across the entire pH range but become noisier under alkaline conditions. This suggests that surface copper is not oxidized but that the signal is diminished as an Fe-oxide coating forms at high pH.

et al. (1996) proposed that the mineral surface comprised ferric or cupric oxides/hydroxides at pH 10. Buckley and Woods (1984) and Zachwieja (1989) observed the formation of a hydrated iron oxyhydroxide layer and an iron-deficient chalcopyrite lattice in air-saturated alkaline solutions. A similar trend in the nature of the surface product with pH was reported by Yin et al. (1995), who found that electrochemical oxidation of chalcopyrite depends on pH, with the formation of sulfate being replaced by that of iron oxide or hydroxide as the pH increased.

3.2.2. XES

We collected O K-edge XES to further elucidate the nature of the surface products of chalcopyrite oxidation. O K-edge XES is a good probe of surface oxidation products because there is no contribution from the bulk mineral. XES spectra were taken at excitation energies corresponding to the peaks in the O K-edge XAS spectra (represented as arrows in Fig. 6).

At low pH, 1.85 (Fig. 6a), all the XES spectra display a small peak at 521 eV, and a dominant peak at 525.5 eV. Because no oxide contribution was seen in the O K-edge XAS, these two peaks may be sampling hydroxide and sulfate, respectively. This is consistent with our conclusion that a (hydroxy)sulfate, such as jarosite, is present in the surface oxidation layer. The individual hydroxide and sulfate contributions were not resolved in the XAS spectra, however, as the transition energy between the O (1s) orbitals of OH^- and

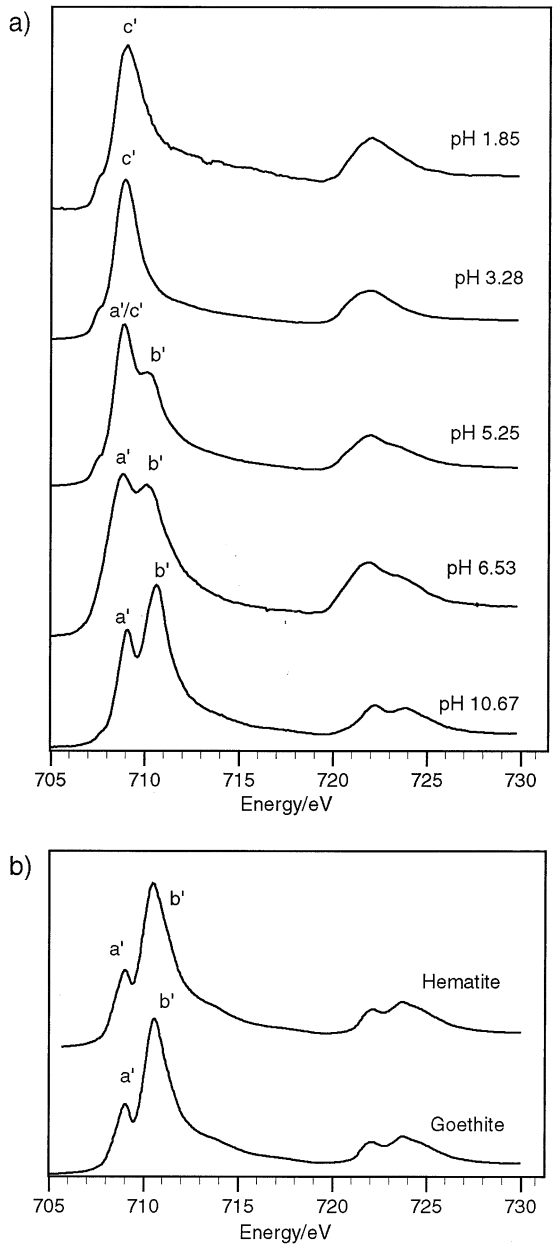

Fig. 4. (a) The Fe L-edges of chalcopyrite samples conditioned in $NaNO_3$ at a range of pH. At low pH, the spectra have a single broad peak, comparable to that of the bulk mineral. Above pH 5, the spectra change markedly and consist of two split peaks corresponding to the 3d t_{2g}- and e_g-states of octahedral Fe (III). This indicates a transition from primarily bulk Fe (II) under acidic conditions (mildly oxidized surface) to an extensively oxidized surface under alkaline conditions. The proportion of Fe (III) increases as the pH rises, and the spectra are consistent with an iron (III) (oxyhydr)oxide surface species, such a goethite, α-FeOOH. (b) The Fe L-edges of iron oxide, hematite and iron (oxyhydr)oxide goethite. The spectra show the characteristic splitting of the L_3- and L_2-edges, attributed to excitations from the Fe (III) (2p) states to Fe (III) t_{2g}- and e_g-like states. This is typical of iron (III) in octahedral coordination.

the metal 3d orbitals in the Fe-OH bond is of a similar magnitude to the same transition in SO_4^{2-}.

At intermediate pH, 6.53, the spectra (Fig. 6b) also show no

Table 3. Peak energies and assignments in O K-edge spectra.

Peak	Energy/eV	Peak assignment	Example minerals
a	530.2 eV	O (1s) in $O^{2-} \Rightarrow t_{2g}$ Fe (3d)-like states in Fe (III)-O	Hematite, goethite (octahedral ferric oxides); high pH/air oxidation chalcopyrite
b	531.6 eV	O (1s) in $O^{2-} \Rightarrow e_g$ Fe (3d)-like states in Fe (III)-O	Hematite, goethite (octahedral ferric oxides); high pH/air oxidation chalcopyrite
c	531.9 eV	O (1s) in $SO_4^{2-} \Rightarrow$ Fe/Cu (3d)-like states	Ferric sulfate Copper sulfate Low pH oxidation chalcopyrite
d	533 eV	O (1s) in $OH^- \Rightarrow$ Fe (3d)-like states	Goethite (hydroxide component) High pH/air oxidation chalcopyrite
e	~534 eV	O (1s) in $OH^- \Rightarrow$ O (2p)-H (1s) antibonding molecular orbital in OH^-	Adsorbed water?
f	537.6 eV	O (1s) in $SO_4^{2-} \Rightarrow$ S (3p, 4s)-O (2p) antibonding molecular orbital in SO_4^{2-}	Ferric sulfate Copper sulfate Low pH oxidation chalcopyrite
g	532.3 eV	O (1s) $\Rightarrow$ Cu (3d, 4s)-like states in Cu (I)-O	Cuprite
h	530.2 eV	O (1s) in $O^{2-} \Rightarrow e_g$ Cu (3d)-like states in Cu (II)-O	Tenorite
i	534.7 eV	O (1s) $\Rightarrow$ Cu (4s, 4p)-like states in Cu (II)-O	Tenorite
j	539.0 eV	O (1s) $\Rightarrow$ Cu (4s, 4p)-like states in Cu (II)-O	Tenorite

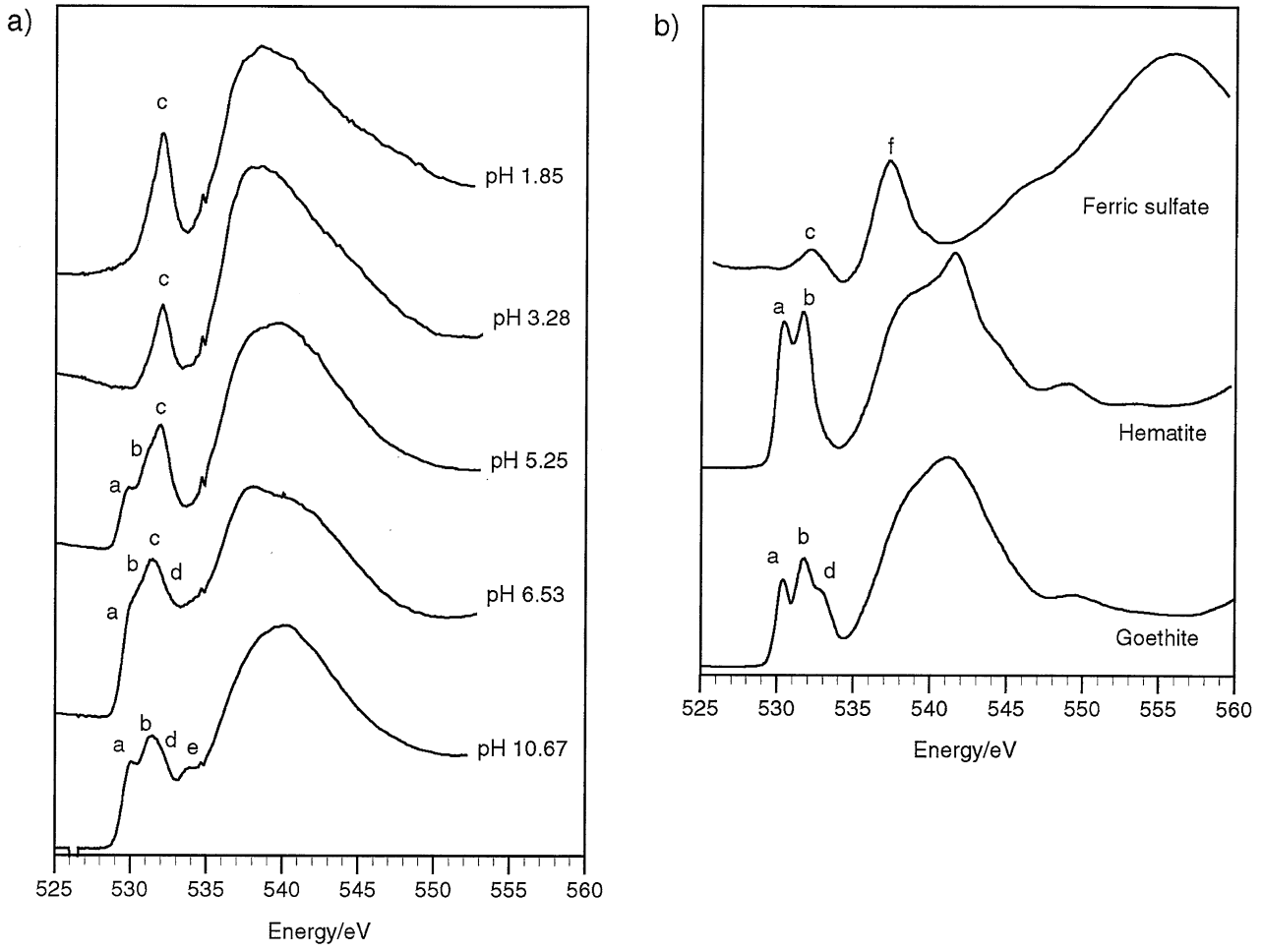

Fig. 5. (a) The oxygen K-edges of a series of chalcopyrite samples conditioned in $NaNO_3$ electrolyte at a range of pH. Mirroring the pattern observed in the Fe L-edges, the O K-edges show a change between pH 3.28 and 5.25, with a single peak attributed to excitations from O (1s) states of oxygen in sulfate to an Fe (3d)-O (2p) state of ferric (hydroxy)sulfate, being replaced by additional peaks at lower energy. The latter are attributed to excitations from O (1s) states of oxygen in oxide to Fe (III) t_{2g}- and e_g-like states of ferric iron as iron (III) (oxyhydr)oxide becomes more stable with rising pH. (b) The O K-edges of ferric sulfate, hematite and goethite. Peaks a and b are excitations from the O (1s) to the t_{2g}- and e_g-like states of Fe (III) in ferric oxide. Peak c is the O (1s) to Fe (3d)-like transition in sulfate. Peak d represents excitations from the O (1s) level of oxygen in hydroxide to the Fe (3d)-like levels. Peak f is assigned to transitions from the O (1s) to S (3p-4s)-O (2p) antibonding orbital of sulfate.

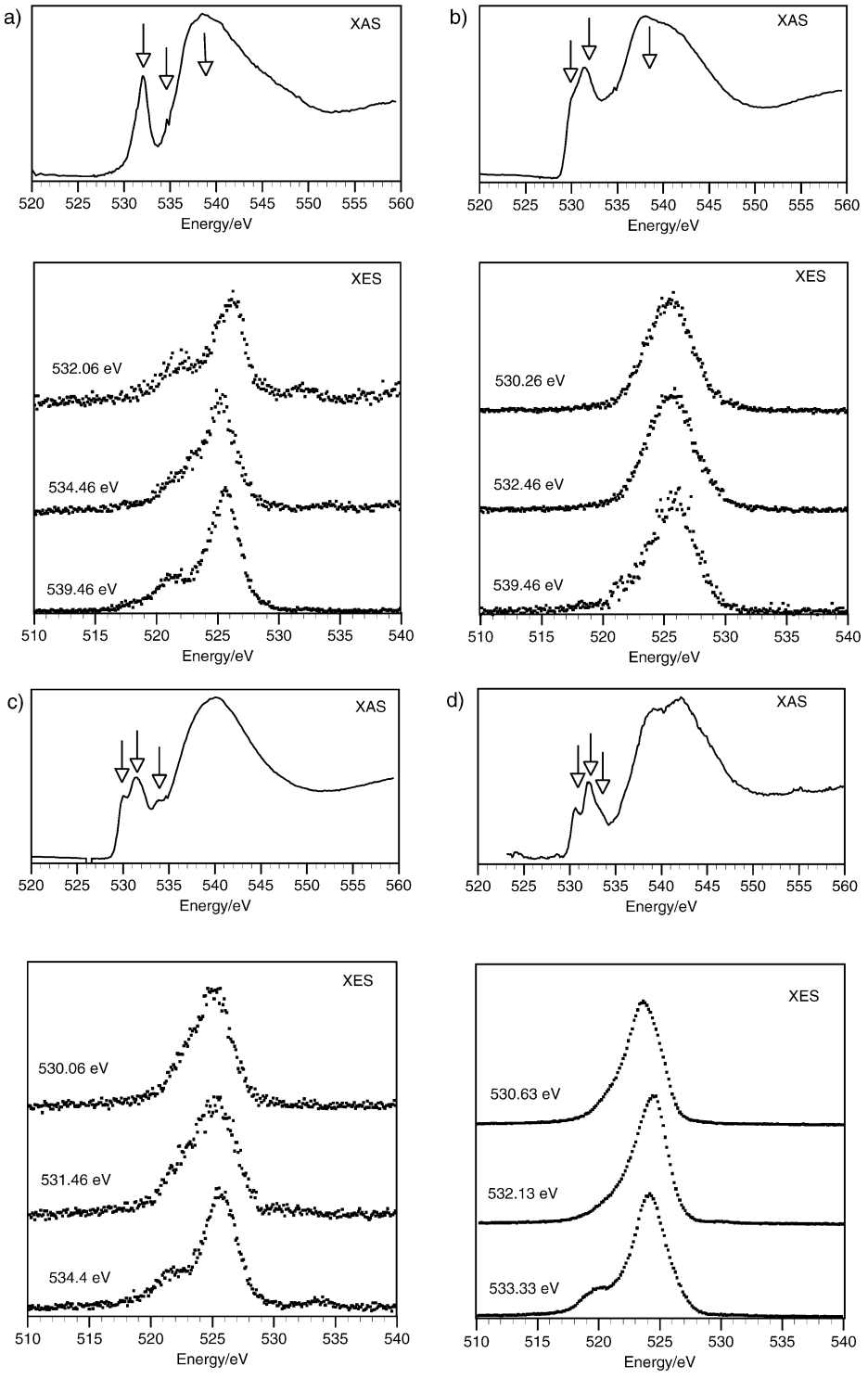

Fig. 6. (a) The O K-edge x-ray emission spectra (XES) of chalcopyrite conditioned in aqueous solution at pH 1.85. Arrows show excitation energies in the O K-edge x-ray absorption spectra (XAS). XES spectra sample occupied states of oxygen 2p character. (b) XES for sample at pH 6.53. (c) XES for sample at pH 10.67. (d) XES of goethite.

excitation energy dependence, but the O K-edge XES now consist of a single peak at 525.5 eV. This is consistent with the presence of an oxide species with a single type of oxygen site, such as oxide, O^{2-}, in Fe_2O_3. The spectra are similar to those of hematite, Fe_2O_3, (Sherman et al., unpublished). Fe_2O_3 may be the dominant surface product, although this conflicts with the corresponding XAS data (Fig. 5). It is possible that we are simply not resolving contributions from oxygen in OH^-.

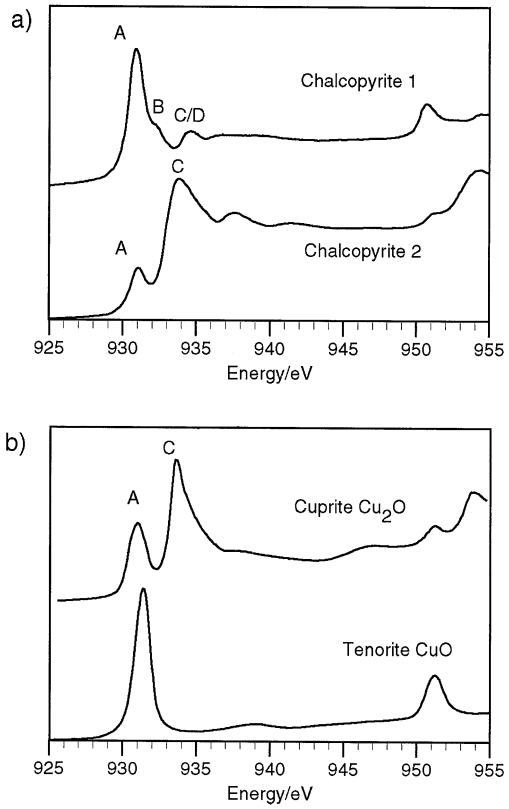

Fig. 7. (a) The Cu L-edges of air-oxidized chalcopyrite. For the oxidized samples, the initial peak (A) is a Cu (II)-O contribution. The shoulder (B) is remnant bulk Cu (II)-S. Peak C corresponds to Cu (I)-O. The surface is extensively oxidized and comprises both Cu (I) and Cu (II) oxides. (b) The Cu L-edges of cuprite, Cu_2O, and tenorite, CuO. For cuprite there are no unoccupied 3d-states, so we would not expect to see a Cu L-edge. The asymmetric peak (C), however, represents the Cu (I) (2p) to Cu (I) (3d-4s) transition and is allowed due to 3d-character in the unoccupied states, resulting from 3d-4s hybridization. The first peak (A) is Cu (II)-O contamination. The tenorite spectrum shows transitions from the Cu (II) (2p) to Cu (II) (3d) states.

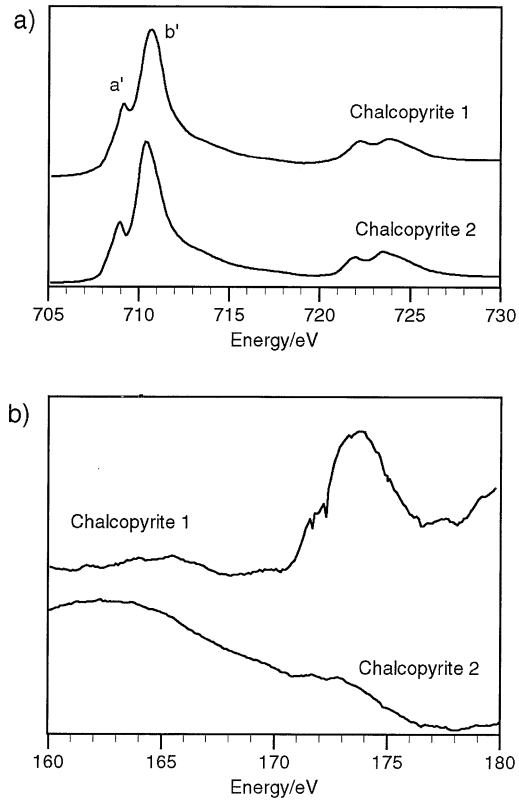

Fig. 8. (a) The Fe L-edges of air-oxidized chalcopyrite. The dominant surface iron state for oxidized chalcopyrite is octahedral Fe (III). This is consistent with the presence of an iron (III) (oxyhydr)oxide or sulfate. (b) The S L-edges of air-oxidized chalcopyrite. The spectrum of the oxidized surface is dominated by a broad feature around 173.4 eV. This indicates the presence of sulfate on the mineral surface.

Under strongly alkaline conditions, the most likely surface oxidation species, based on the XAS data (Fig. 5), is an iron (oxyhydr)oxide such as goethite. This is verified by the XES data (Fig. 6c). Excitation at 533.86 eV yields both a 525.5 eV emission and a peak at 521.8 eV. The latter corresponds to oxygen present as hydroxide, OH^-, as seen in the reference spectrum of goethite obtained at ALS (Fig. 6d). On variation of the excitation energy, the spectra selectively sample first the oxide, and then the oxide + hydroxide components in the surface, each having different binding energies. Thus the change in the XES spectra with excitation energy reveal the presence of inequivalent oxygen sites (oxide and hydroxide) in an iron (III) (oxyhydr)oxide oxidation species such as goethite, consistent with the earlier conclusions based on XAS data.

3.3. Air Oxidation of Chalcopyrite

3.3.1. XAS spectroscopy

Cu, Fe, and S L-edge, and O K-edge spectra were collected for two chalcopyrite samples oxidized under ambient atmospheric conditions (T = 20°C, P_{H2O} ~0.02 bar) for at least 7 days.

For both chalcopyrite samples the copper L-edge (Fig. 7a) has a feature at 931.4 eV (peak A). This correlates with the Cu (2p) → Cu (3d)-like transition in CuO (Fig. 7b); indicating that there has been a change in coordination from surface Cu (II)-S to Cu (II)-O. In one sample the small peak (B) at 932.3 eV is assigned to an excitation to the Cu (3d)-like states of the bulk Cu^{2+}bonded to sulfur, as seen in the corresponding spectrum of covellite (Fig. 2a). The asymmetric peak at about 953.6 eV coincides with a similar feature in the Cu L-edge spectra of Cu_2O (Fig. 7b) and Cu_2S (Fig. 2a). This feature is attributed to the 2p-3d channel of Cu (I) and results from 3d-4s hybridization (Grioni et al., 1989b). The presence of Cu (I) oxides indicates that there must be some surface disproportionation occurring to give a mixture of copper (I) and copper (II) oxides, with the relative proportions of each depending on the extent of oxidation.

The Fe L-edges (Fig. 8a) of both oxidized chalcopyrite samples reveal that iron species are present in the Fe (III) state, with split peaks (a′ and b′) present in the L_3-edge at 709 and 710.5 eV. This is characteristic of all the iron (III) (oxyhydr)-oxides studied and is attributed to the splitting of the Fe (III) (3d) orbital due to octahedral coordination with oxygen.

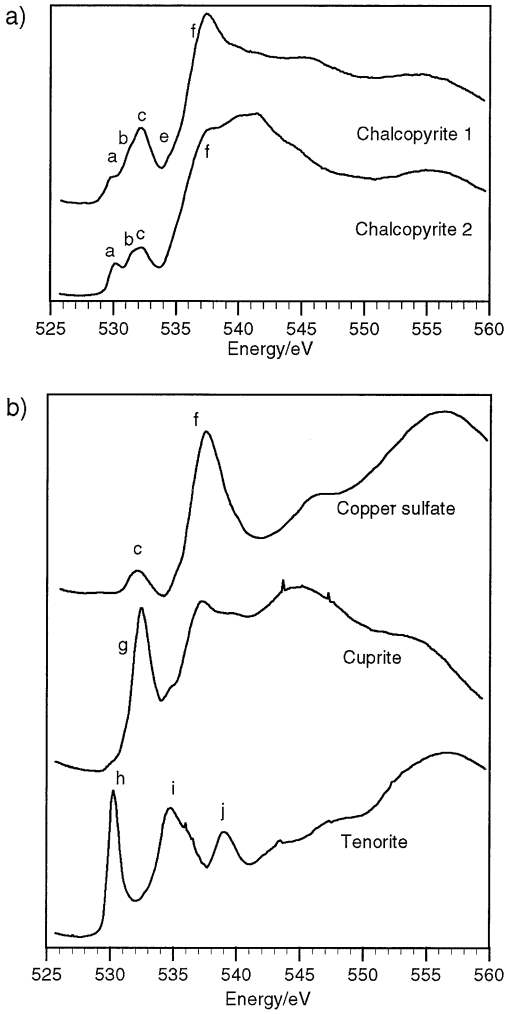

Fig. 9. (a) The OK-edges of air-oxidized chalcopyrite. The spectra have a complex low-energy structure, indicating the presence of various surface oxide phases. Unfortunately, the Cu 3d- and Fe 3d-states lie at similar binding energies and cannot be distinguished. Peak f, however, reveals the presence of sulfate. (b) The O K-edges of copper sulfate, cuprite, and tenorite references. Copper sulfate has a main peak (f), which is assigned to transitions from the O (1s) to S (3p, 4s)-O (2p) antibonding orbital. The small pre-edge peak (c) is the O (1s) to Cu (3d)-O (2p) transition. For cuprite, the absence of a pre-edge peak is compatible with the fully-occupied d^{10} electronic structure. The strong pre-edge peak (h) in tenorite indicates a transition to unoccupied 3d-like states of Cu (II)-O.

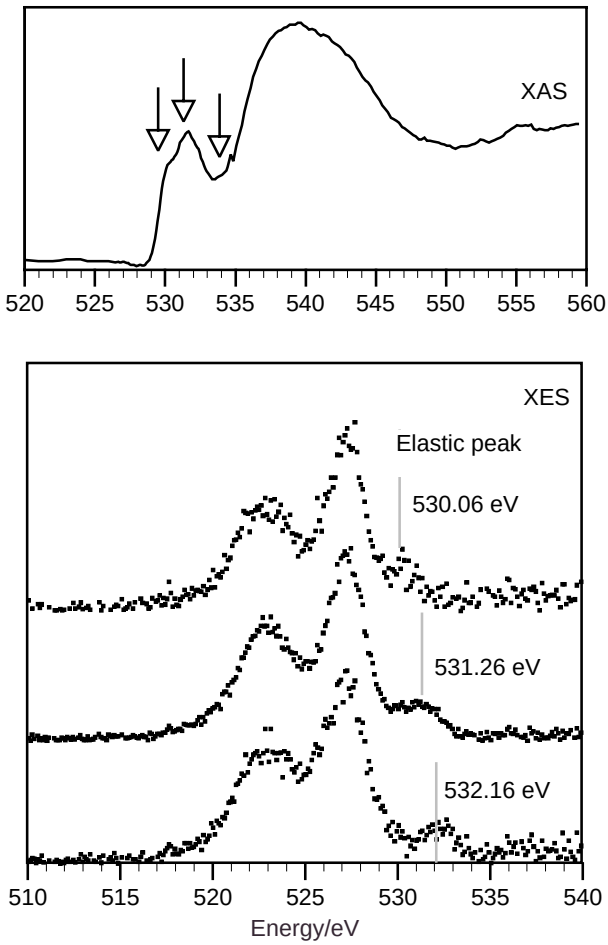

Fig. 10. The O K-edge XES of air-oxidized chalcopyrite. Similarly to the XES spectrum of chalcopyrite oxidized in acidic aqueous solution, the spectra have a double-peaked structure at all excitation energies. This may be indicative of sulfate on the mineral surface. The smaller peak ratio however, probably means that there are additional contributing species, compatible with the surface being a complex mixture of copper and iron (oxyhydr)oxide and sulfate oxidation products.

The S L-edges of air-oxidized chalcopyrite (Fig. 8b) have a broad peak at about 173.5 eV, attributed to the presence of sulfate in the surface oxidation layer. The XPS observations of Buckley and Woods (1984) also showed that sulfate can form, along with Cu (II) species after prolonged air oxidation of the chalcopyrite surface.

The oxygen K-edges of air-oxidized chalcopyrite (Fig. 9a) are complex and probably have contributions from both copper and iron oxidation products. Between 528 and 534 eV there are numerous peaks buried in a broad feature, corresponding to transitions to the Fe (3d)-like orbitals of ferric iron and the Cu (3d, 4s)-like orbitals of Cu (I) and Cu (II). The surface is probably heterogeneous and composed of a complex mixture of iron and copper oxides and sulfates. The presence of sulfates is indicated by the strong peak (f) at 537.5 eV in both chalcopyrite samples. This can be assigned to the same O (1s) $\rightarrow$ S (3p, 4s)-O (2p) transition as in the O K-edge spectra of both ferric and cupric sulfate (Figs. 5b and 9b).

3.3.2. XES

The O K-edge X-ray emission spectra of air-oxidized chalcopyrite (Fig. 10) show a double-peaked structure, but the intensity ratio of the two peaks is much lower than that displayed by any of the aqueous samples. Both features are present at all excitation energies. Although the O K-edge XAS spectrum for air-oxidized chalcopyrite resembles closely that of iron (III) (oxyhydr)oxide (Fig. 5b), the XES reveal that this is not the only species present. Because goethite contains two oxygen types (O^{2-} and OH^{-}), we would expect to see a strong excitation energy dependence of the spectra (see Fig. 6d).

Instead, the double-peaked structure is present at all excitation energies. This suggests that there is at least one other species present. The low-pH aqueous sample (Fig. 6a) also showed a double-peaked structure (attributed to sulfate and OH^- oxygen). Hence, we conclude that the air-oxidized chalcopyrite surface consists of both sulfate and oxy(hydroxide) species. Buckley and Woods (1984) suggested that initial iron hydroxide formation is followed by the appearance of iron sulfate, with a CuS layer developing beneath the uppermost surface. Pratesi and Cipriani (2000) have also suggested that the surface oxygen contribution is provided by both iron and copper sulfates. The oxidized surface is obviously heterogeneous and contains various metal oxide and sulfate species. Unfortunately, the individual features cannot be distinguished in the XES spectra.

4. CONCLUSIONS

The surface oxidation layer on chalcopyrite in aqueous solution changes markedly with pH. Under strongly acidic conditions, the surface phase appears to be a ferric (hydroxy)sulfate. At high pH, the major surface phase is an iron (oxyhydr)oxide, probably goethite. The spectra demonstrate a progressive transition between these species as the pH is raised. Copper is not present in the surface oxidation layer. Soluble copper oxidation products may be leached from the surface and go into solution.

For air-oxidized chalcopyrite, the O K-edge XAS spectra again show the presence of iron (III) (oxyhydr)oxide species but, in this case, the copper L-edges reveal that the surfaces also contain copper oxidation products, in contrast to the aqueous samples. Sulfate is revealed as an important species in the S L-edge spectra. The XES spectra also point to a complex oxidized surface, probably consisting of a mixture of CuO (tenorite), FeOOH (goethite), copper and/or ferric iron sulfates, and possibly Cu_2O (cuprite) or Cu_2S (chalcocite) surface species. Sulfate may be less significant on the surfaces of aqueous chalcopyrite samples compared with those oxidized in air because of its high solubility in water.

Acknowledgments—This work was made possible by direct access from CLRC, Daresbury Laboratory, ARI economic support through Max Lab, and NERC. ECT is supported by a NERC studentship. The authors would also like to thank J. Denlinger of the Advanced Light Source, Lawrence Berkeley National Laboratory, and A. Augustsson, T. Schmitt, F. Trif (Uppsala University), and L. Gridneva at Max Lab., Lund, Sweden, for their assistance with XAS and XES spectroscopy. We are also grateful for the comments of three anonymous reviewers.

REFERENCES

Abbate M., Goedkoop J.B., Degroot F.M.F., Grioni M., Fuggle J.C., Hofmann S., Petersen H., and Sacchi M. (1992) Probing depth of soft-X-ray absorption-spectroscopy measured in total-electron-yield mode. *Surf. Interface Analysis* **18,** 65–69.

Brion D. (1980) Photoelectron spectroscopic study of the surface degradation of pyrite (FeS_2), chalcopyrite ($CuFeS_2$), sphalerite (ZnS), and galena (PbS) in air and water. *Appl. Surf. Sci.* **5,** 133–152.

Buckley A. N. and Woods R. (1984) An X-ray photoelectron spectroscopic study of the oxidation of chalcopyrite. *Aust. J. Chem.* **37,** 2403–2413.

Gardner J. R. and Woods R. (1979) An electrochemical investigation of the natural flotability of chalcopyrite. *Int. J. Miner. Process.* **6,** 1–18.

Grano S. R., Sollaart M., Skinner W., Prestidge C. A., and Ralston J. (1997) Surface modifications in the chalcopyrite-sulfite ion system. I. collectorless flotation, XPS and dissolution study. *Int. J. Miner. Process.* **50,** 1–6.

Grioni M., Goedkoop J. B., Schoorl R., de Groot F. M. F., Fuggle J. C., Schafers F., Koch E. E., Rossi G., Esteva J.-M., and Karnatak R. C. (1989) Studies of copper valence states with Cu L3 x-ray absorption spectroscopy. *Phys. Rev. B.* **39,** 1541–1545.

Helgeson H. C., Delany J. M., Nesbitt H. W., and Bird D. K. (1978) Summary and critique of the thermodynamic properties of rock-forming minerals. *Amer. J. Sci* **278,** 229.

Kasrai M., Lennard W. N., Brunner R. W., Bancroft G. M., Bardwell J. A., and Tan K. H. (1996) Sampling depth of total electron and fluorescence measurements in Si L- and K-edge absorption spectroscopy. *Appl. Surf. Sci.* **99,** 303–312.

Li D., Bancroft G. M., Kasrai M., Fleet M. E., Yang B. X., Feng X. H., Tan K., and Peng M. (1994a) Sulfur K- and L-edge absorption spectroscopy of sphalerite, chalcopyrite and stannite. *Phys. Chem. Miner.* **20,** 489–499.

Li D., Bancroft G. M., Kasrai M. E., Fleet M. E., Feng X. H., Yang B. X., and Tan K. H. (1994b) S K- and L-edge XANES and electronic structure of some copper sulfide minerals. *Phys. Chem. Miner.* **21,** 317–324.

Luttrell G. H. and Yoon R. H. (1984) Surface studies of the collectorless flotation of chalcopyrite. *Colloid Surf.* **12,** 239–254.

Mielczarski J. A., Cases J. M., Alnot M., and Ehrhardt J. J. (1996) XPS Characterization of chalcopyrite, tetrahedrite and tennantite surface products after different conditioning.1. Aqueous solution at pH 10. *Langmuir* **12,** 2519–2530.

Myneni S., Luo Y., Naslund L. A., Cavalleri M., Ojamae L., Ogasawara H., Pelmenschikov A., Wernet P., Vaterlein P., Heske C., Hussain Z., Pettersson L. G. M., and Nilsson A. (2002) Spectroscopic probing of local hydrogen-bonding structures in liquid water. *J. Phys. Condens. Matter* **14,** L213–L219.

Pattrick R. A. D., van der Laan G., Vaughan D. J., and Henderson C. M. B. (1993) Oxidation state and electronic configuration determination of copper in tetrahedrite group minerals by L-edge X-ray absorption spectroscopy. *Phys. Chem. Miner.* **20,** 395–401.

Pattrick R. A. D., Mosselmans J. F. W., Charnock J. M., England K. E. R., Helz G. R., Gardner C. D., and Vaughan D. J. (1997) The structure of amorphous copper sulfide precipitates: An X-ray absorption study. *Geochim. Cosmochim. Acta* **61,** 2023–2036.

Pratesi G. and Cipriani C. (2000) Selective depth analyses of the alteration products of bornite, chalcopyrite and pyrite performed by XPS, AES and RBS. *Eur. J Mineralol.* **12,** 397–409.

van der Laan G., Pattrick R. A. D., Henderson C. M. B., and Vaughan D. J. (1992) Oxidation state variations in copper minerals studied with Cu 2p X-ray absorption spectroscopy. *J. Phys. Chem. Solids* **53,** 1185–1190.

Vaughan D. J. and Craig J. R. (1978) *Mineral Chemistry of Metal Sulfides.* Cambridge University Press.

Vaughan D. J., England K. E. R., Kelsall G. H., and Yin Q. (1995) Electrochemical oxidation of chalcopyrite (CuFeS2) and the related metal-enriched derivatives $Cu_4Fe_5S_8$, $Cu_9Fe_9S_{16}$ and $Cu_9Fe_{8S}S_{16}$. *Am Miner.* **80,** 725–731.

Velasquez P., Gomez H., Ramos-Barrado J. R., and Leinen D. (1998) Voltammetry and XPS analysis of a chalcopyrite $CuFeS_2$ electrode. Colloids and Surfaces A: Physicochemical and Engineering Aspects **140,** 369–375.

Wagman D. D., Evans W. H., Parker V. B., Schumm R. H., Halow I., Bailey S. M., Churney K. L., and Nuttall R. L. (1982) The NBS tables of chemical thermodynamic properties, selected values for inorganic and c1 and c2 organic substances in SI units. *J. Phys. Chem. Ref. Data* **11,** 392.

Yin Q., Kelsall G. H., Vaughan D. J., and England K. E. R. (1995) Atmospheric and electrochemical oxidation of the surface of chalcopyrite ($CuFeS_2$). *Geochim. Cosmochim. Acta.* **59,** 1091–1100.

Zachwieja J. B., McCarron J. J., Walker G. W., and Buckley A. N. (1989) Correlation between the surface composition and collectorless flotation of chalcopyrite. *Colloid Interface Sci.* **132,** 462–468.